

Double proton shifts in associates of formic acid with CH_4 , NH_3 , H_2O , CH_3F , NH_2F , HOF , and HF molecules*

R. M. Minyaev* and V. I. Minkin

Institute of Physical and Organic Chemistry at Rostov State University,
194/3 prosp. Stachki, 344104 Rostov-on-Don, Russian Federation.
Fax: +7 (863 2) 28 5667

The mechanisms of double synchronous proton transfer in associates of formic acid with solvent molecules of the $\text{HC}(\text{O})\text{OH}\cdots\text{X}$ ($\text{X} = \text{CH}_4$, NH_3 , H_2O , or HF) and $\text{HC}(\text{O})\text{OH}\cdots\text{FH}\cdots\text{Y}$ ($\text{Y} = \text{CH}_3\text{F}$, NH_2F , HOF , F_2 , or HF) types have been studied by an *ab initio* (SCF/3G) method. The calculated activation barriers of the reactions are 78.52, 17.72, 9.91, and 7.06 kcal mol⁻¹ in the former case and 120.1, 259.4, 228.7, 182.8, and 0.35 kcal mol⁻¹ in the latter case. In the latter case, simultaneously with the double transfer of protons, migration of two fluorine atoms along the chain of the associate occurs.

Key words: formic acid, associate; potential energy surface; reaction pathway; energy barrier of reaction.

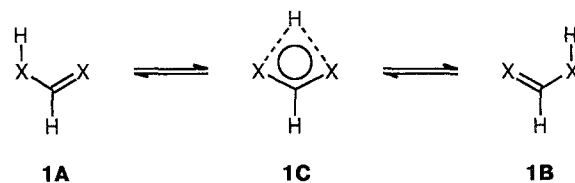
To understand the mechanisms of the reactions occurring in enzymatic systems and the dynamics of their functioning, simulation of these reactions using simple molecular systems that adequately reflect basic dynamic characteristics of cooperative processes is often required. Intermolecular proton transfers play one of the leading parts in these processes.¹⁻⁷ The height of the energy barrier to the proton transfer is mostly determined by the following factors: (1) fulfillment of the steric requirement that the geometry of the $\text{X}\cdots\text{H}\cdots\text{Y}$ hydrogen bond be sufficiently close to the optimal linear configuration of the three-center bridge; (2) the acidity (the energy of heterolytic dissociation) of the $\text{Y}-\text{H}$ bond; (3) the basicity of the proton accepting center X ; (4) the electron delocalization (quasiaromatic character) of the ring that is closed through the hydrogen bond in the case when X and Y are parts of the same molecule (intramolecular hydrogen bond).^{1,7-9}

If the system does not comply with one or more of the foregoing requirements, the proton transfer is accompanied by overcoming a rather high activation barrier. In fact, intramolecular migrations (1,3-shifts) of protons (Scheme 1) in molecules of formamidine (**1A**, $\text{X} = \text{NH}$) and formic acid (**1A**, $\text{X} = \text{O}$), according to experimental data and results of quantum-chemical calculations,¹⁻³ are associated with climbing over rather high activation barriers (>40 kcal mol⁻¹). However, as shown by *ab initio* calculations, intermolecular transfer of protons in dimers of carboxylic acids and amidines (eight-membered rings)¹ and also in associates of the latter with one H_2O molecule (six-membered rings formed by hydrogen

bonds)^{3,4} is substantially facilitated (Scheme 2) and involves activation barriers that are only one half or one third of those in the case of intramolecular processes.

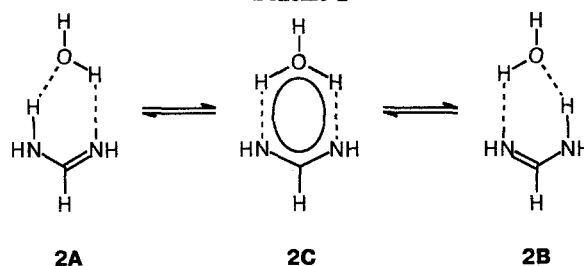
This substantial decrease in the barriers to hydrogen transfer is obviously due to the fact that steric conditions in associates **2** are more favorable for H-bridges to close and for protons to move along them than those in **1**. Therefore, these reactions (see Scheme 2) may serve as a base of processes of bifunctional catalysis, enzymolysis, and tautomerization promoted by water molecules, despite the fact that they require two synchronous proton migrations.^{1,10} However, general regularities, associated with the nature of one-step (concerted) transfer of two

Scheme 1



$\text{X} = \text{NH}, \text{O}$

Scheme 2



* Dedicated to Academician of the RAS N. S. Zefirov (on his 60th birthday).

or more protons between reaction contacts in a complex molecular system, are not yet entirely known. Along with water molecules, other molecules containing Y—H type bonds can act as proton-transferring species. It is of interest to find out, what structure of associates incorporating these molecules would ensure the occurrence of low-barrier proton transfer. Reactions of this type are an important step or are involved in cooperative transformations that occur in substrate—enzyme complexes and, as a rule,¹¹ along with the transfer of protons, they include the transfer of one or several multielectron groups between reaction centers.

The main purposes of the present work have been to study the effect of CH₄, NH₃, H₂O, and HF molecules, which simulate proton-donating and proton-withdrawing media, whose basicity and acidity vary over wide limits, on the height of the energy barrier to the 1,3-transfer of protons in associates **3** with formic acid molecules, according to Scheme 3, and also to study the effect of the incorporation of the second transferring molecule, HF, on the mechanism and kinetics of the proton shift in the model reaction (Scheme 4) in which double proton migrations are accompanied by synchronous displacements of the two fluorine atoms from one solvent molecule to another, using *ab initio* calculations.

Determination of precise quantitative characteristics of proton shifts was not our task. Therefore, the reactions shown in Schemes 3 and 4 were studied by the *ab initio* (SCF) method in the minimum STO-3G basis

set.¹² Although this basis set is insufficient to predict precise geometric and energetic properties of the systems under consideration, it has proved to be satisfactorily applicable and reliable for qualitative analysis of the topology of the potential energy surface (PES) and the pathways of double shifts of protons in neutral systems.^{1,7,12,13}

Procedure of the Calculations

Calculations were carried out on AST Premium/386C and PC-486 personal computers by the restricted Hartree—Fock (SCF/3G) method¹² using the MICROMOL-5 program.¹⁴ The STO-3G basis set is insufficient to obtain quantitative estimates for anionic structures; in this case, to achieve satisfactory agreement with experimental data, one should use valence-split sets that necessarily include polarization functions.^{1,12} Therefore, in the present work for the calculations of anionic forms, the STO-6-31G* basis set (see Ref. 12) was used.

Full optimization of the geometry of molecular structures corresponding to the saddle points ($\lambda = 1$; hereinafter, λ is the number of negative eigenvalues of the Hesse matrix in the given critical point^{1,15}) was carried out up to a gradient magnitude of 10^{-6} au B⁻¹, and that for the molecular structures corresponding to the energy minima ($\lambda = 0$) on the PES was carried out up to 10^{-3} au B⁻¹, due to the extremely slow convergence of the optimization process. The matrix of force constants was calculated numerically according to the three-point scheme with a step of 0.001 Å using a MICROMOL program.

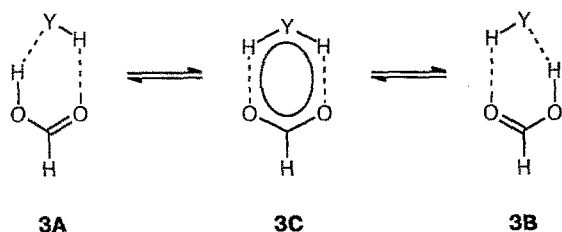
The structures corresponding to the energy minima on PES were found by the method of steepest descent (movement along the gradient line) from a saddle point (transition state) to the neighboring critical point (a saddle point or a maximum), which simultaneously recorded the gradient reaction pathway,¹⁵ connecting minima to the corresponding saddle points. The initial direction of the gradient line was specified by a minor displacement along the direction of the transition vector of the corresponding transition structure.

The superposition error in the calculations of the energies of stabilization of associates with respect to the separate molecules of formic acid and the solvent was not taken into account, since we mostly studied interassociate reaction pathways, rather than dissociation limits, for which the allowance for this error would have been especially important.¹² We also did not consider the influence of tunnel effects on the mechanisms and energetics of the reactions under study, since one may expect that these effects are negligibly small owing to the substantial contribution of the motion of all of the multielectron atoms to the reaction coordinate.¹⁶

Results and Discussion

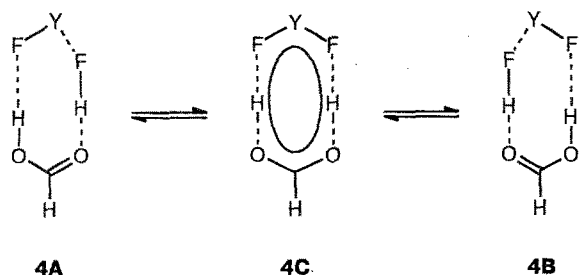
Proton transfer by the electrophilic substitution mechanism (S_E2) at the central atom of the solvent (see Scheme 3). The calculations have shown that all of associates **3A** correspond to energy minima ($\lambda = 0$), and symmetrical structures **3C** correspond to saddle points ($\lambda = 1$) on the PES. The energetic and geometric characteristics of the ground and transition states **3A** and **3C** calculated are presented in Table 1 and in Figs. 1 and 2, respectively.

Scheme 3



Y = Me (a), NH₂ (b), OH (c), F (d)

Scheme 4



Y = Me (a), NH₂ (b), OH (c), F (d), H (e)

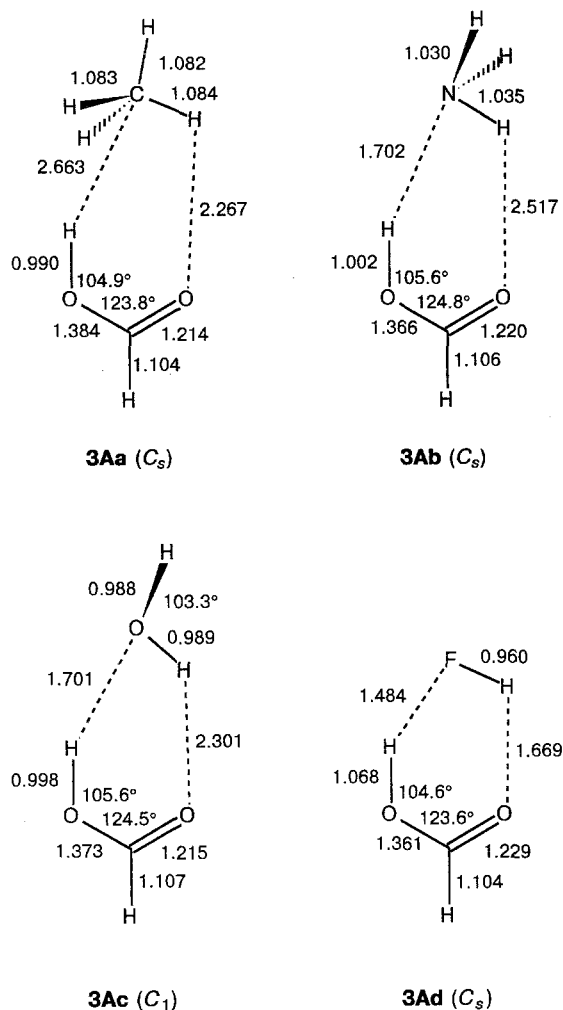


Fig. 1. Structures of associates **3A** calculated by the SCF/3G method. Bond lengths (in Å) and angles are presented.

Associates **3A** are prereaction complexes stabilized by the formation of hydrogen bonds between the molecules of formic acid and the solvent (see Fig. 1). However, the superposition error,¹² which may be as high as ~1–5 kcal mol⁻¹ in minimum basis sets, has not been taken into account in these calculations, therefore, the values obtained for the energies of hydrogen bonds should be treated with caution. This is especially true for the energy, predicted for the weak hydrogen bond (~0.2 kcal mol⁻¹) between the molecules of formic acid and methane in associate **3Aa**.

For low-barrier intramolecular rearrangements to occur, the principle of stereochemical correlation between the transition state of the given reaction and transition states of "elementary" reactions must be fulfilled.^{9,17} The 1,3-transfer of a proton (see Scheme 3) occurs *via* cyclic transition state **3C** with two bridging hydrogen bonds (see Fig. 2). In this reaction, the solvent molecule accomplishes bifunctional (acid-base) catalysis, acting both as a proton donor and a proton acceptor,

Table 1. Total (E_{total}) and relative (ΔE) energies, number of negative eigenvalues of Hessian (λ), and the two minimum (ν_1 , ν_2) or imaginary (ν) frequencies of associates **3A**, **3C** and individual molecules

Structure	$-E_{\text{total}}$ /au	ΔE^a /kcal mol ⁻¹	λ	ν (ν_1 , ν_2) /cm ⁻¹
3Aa	225.94505	0	0	(62, 93)
3Ab	241.69052	0	0	(90, 131)
3Ac	261.20140	0	0	(91, 205)
3Ad	284.80869	0	0	(265, 270)
3Ca	225.81990	78.52	1	i2633.6
3Cb	241.66228	17.72	1	i1729.5
3Cc	261.18429	10.72	1	i1546.7
3Cd	284.79744	7.06	1	i1455.0
3Ce^b	225.72460	138.33	1	i2953.8
HC(O)OH	186.21788		0	
CH ₄	39.72666	0.20 ^c	0	
NH ₃	55.45542	10.80 ^c	0	
H ₂ O	74.96590	11.04 ^c	0	
HF	98.57285	11.27 ^c	0	

Note. Here and in Tables 2 and 3 the data of *ab initio* calculations in the SCF/3G basis set are presented. ^a 1 au = 627.517 kcal mol⁻¹. ^b Y = Me (see Fig. 2). ^c Relative energies of states with separate molecules of formic acid and the solvent.

and cooperatively transports two protons, synchronously along two hydrogen bridges. This process can be conventionally divided into three "elementary" reactions: (a) transfer of a proton from the O atom of formic acid to the YH molecule; (b) electrophilic substitution of hydrogen at the central atom of the YH molecule; (c) transfer of a proton from the YH molecule to the second O atom of formic acid.

The transfer of a proton from one atom to another is supposed to occur *via* a linear transition state.^{1,7} However, our calculations showed that substantial deviations from linearity (up to 30°) in the F—H—F⁻ structure result in slight variations of the total energy of the system (within 5–10 kcal mol⁻¹). This result is in good agreement with experimental¹⁸ and calculated data⁷ that the energies of hydrogen bonds are not very sensitive to angular deformations within these limits.

The assignment of the second "elementary" reaction to bimolecular electrophilic substitution (S_E2) of hydrogen at the central atom of the solvent molecule, YH, may be reasoned, first, by the fact that the configuration of the Y—H bonds at this atom in transition state **3C** is close to that found for the structures of CH₅⁺ (**5**), NH₄⁺ (**6**), OH₃⁺ (**7**), and FH₂⁺ (**8**) cations (Scheme 5, bond lengths and angles are given), which model the simplest transition states (intermediates) of S_E2 reactions of the period II element hydrides,¹ and, second, by the fact that the migrating protons in transition structures **3C** carry rather large positive charges (Scheme 6, the numbers mean the charges of the corresponding atoms). The decrease in the activation barrier to the 1,3-shift of a

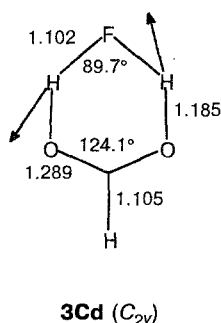
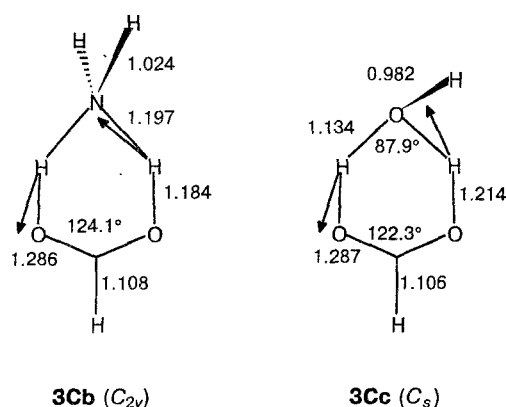
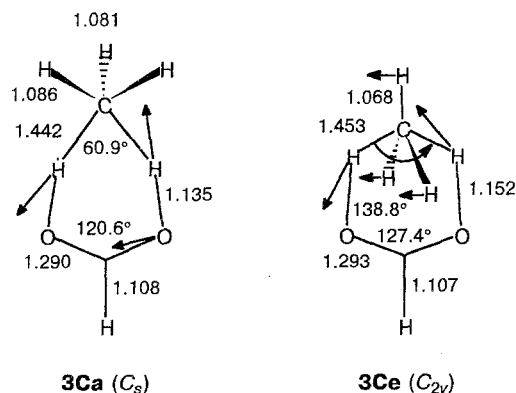
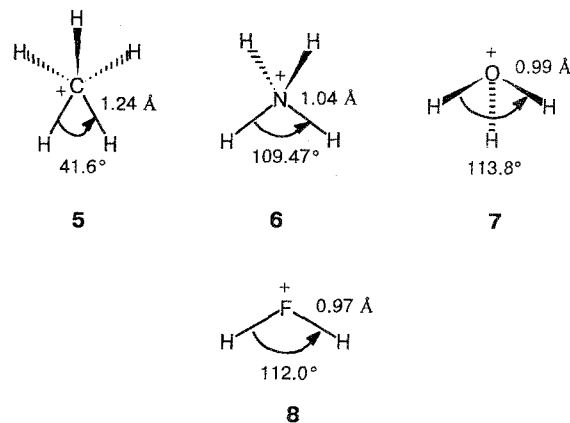


Fig. 2. Structures of transition states **3C** calculated by the SCF/3G method. Bond lengths (in Å) and angles are presented; the arrows denote components of the corresponding transient vectors.

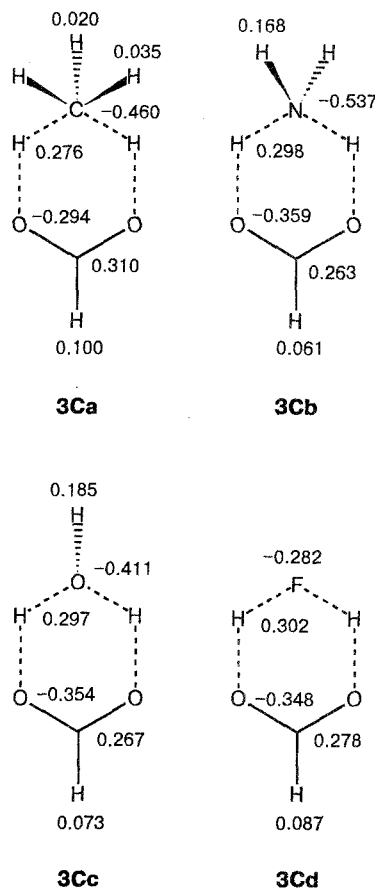
proton in the **3Aa**, **3Ab**, **3Ac**, and **3Ad** series is provided not only by the improvement of the stereochemical correspondence to the similar structures **5–8**, but also by the increase in the electronegativity of the central atom and the acidity of the $Y-H$ bond over this series.

The proton affinity (PA) of the above-mentioned molecules also increases, though not monotonically, over this series. In fact, the SCF/3G-calculated values of proton affinity for CH_4 , NH_3 , H_2O , and FH are 120.1, 259.4, 228.7, and 182.8 kcal mol $^{-1}$, respectively. These values are somewhat higher than the experimental values (PA /kcal mol $^{-1}$: 117.6–122.2 (CH_4), 207.5–

Scheme 5



Scheme 6

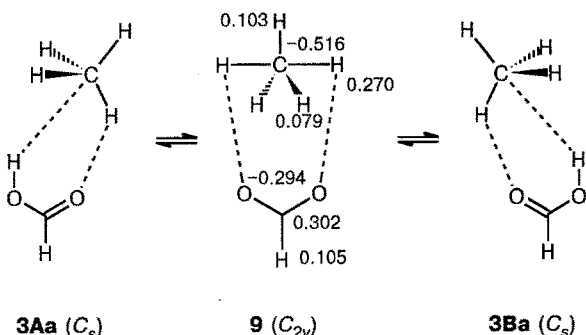


216.8 (NH_3), 153.6–164.6 (H_2O), and 131.4–138.4 (FH))¹⁹; however, they adequately reflect the tendency of their variation for the above-listed molecules.

The process of 1,3-transfer of a proton (see Scheme 3) can be also theoretically represented as bimolecular nucleophilic substitution of hydrogen at the central atom of the proton transferring molecule by setting to this atom the stereochemical configuration associated with this type of reaction. However, in this case, a higher

activation barrier must be overcome, which is due to the fact that the stereochemical correspondence of this unit to the transition state of nucleophilic substitution (S_N2) is considerably worse.^{1,9,20} For example, the activation barrier to the $3Aa \rightarrow 9 \rightarrow 3Ba$ reaction occurring as a nucleophilic process *via* transition state **9** (see Table 1 and Fig. 2) is almost double (138 kcal mol⁻¹) that for the electrophilic mechanism. Besides, despite the fact that the CH_3 unit has the expected trigonal-bipyramidal configuration, the positive charges at the entering and leaving axial hydrogen atoms are larger than those at the equatorial atoms (Scheme 7; the numbers mean the charges at the corresponding atoms).

Scheme 7



This result is in contradiction with the polarity rule,¹ which governs the charge distribution in structures of the trigonal bipyramid type and its derivatives. Thus, transition state **9** is misadjusted both sterically and electronically, which accounts for the fact that it is energetically unfavorable compared to transition state **3Ca**.

The synchronous (concerted) character of the shift of the two protons along the cyclic system is ensured by the formation of multicenter two-electron σ molecular orbitals (MO) in the transition structure **3C**, whose shape for associate **3Cb** is shown in Fig. 3. Any distort-

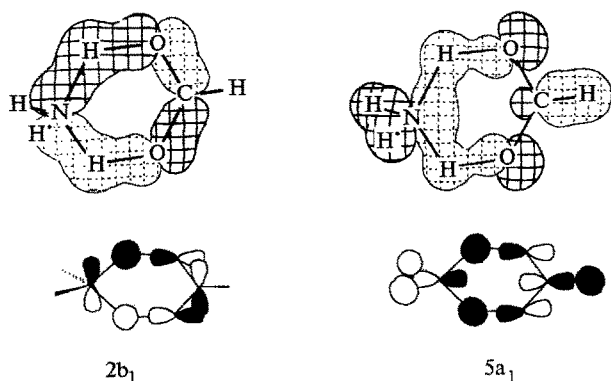


Fig. 3. Molecular orbitals $2b_1$ and $5a_1$ responsible for stabilization of the H-bridges in transition states.

tion of the structure of **3C** toward its disflattening or variation of bond lengths, leading to dissociation into two moieties (stepwise transfer of protons), causes a dramatic increase in the energies of these MO and, consequently, an increase in the total energy of the whole system **3C**.

Proton transfer by the nucleophilic substitution mechanism (S_N2) at the central atom of the solvent (see Scheme 4). If the proton-transferring molecule contains electronegative groups possessing unshared electron pairs (*i.e.*, relatively strong nucleophiles) at the central atom, the transfer of the proton from formic acid may occur *via* nucleophilic substitution step. This case has been considered using type **4** trimolecular systems as an example. As shown by calculations, all of the systems **4A** are associated with energy minima on the PES of the corresponding processes. The calculated energetic and geometric characteristics of systems **4A** and **4C** are given in Figs. 4 and 5, respectively, and in Table 2.

Associates **4A**, like **3A**, are prereaction complexes stabilized through the formation of hydrogen bonds between the molecules of formic acid and the solvent; these bonds are much more strong than those in structures **3A** (see Fig. 4). One may expect that neglect of the superposition error would exert no substantial effect on the strengths of hydrogen bonds for associates **4A** predicted by calculation, except for form **4Ad** ($Y = F$), for which the energy of stabilization obtained by the calculations is too low. It is of interest that, as the results of calculations indicate (see Table 2), a relatively

Table 2. Total (E_{total}) and relative (ΔE) energies, number of negative eigenvalues of Hessian (λ), and the two minimum (v_1 , v_2) or imaginary (iv) frequencies of associates **4A**, transition structures **4C**, and individual molecules

Structure	$-E_{total}$ /au	ΔE^a /kcal mol ⁻¹	λ	iv (v_1 , v_2) /cm ⁻¹
4Aa	421.97719	0	0	(42, 85)
4Ab	437.69913	0	0	(76, 133)
4Ac	457.20648	0	0	(71, 77)
4Ad	480.78110	0	0	(17, 22)
4Ae	383.41568	0	0	(87, 204)
4Ca	421.84180	84.96	1	i1425.1
15a	421.97581	84.96	1	i49.7
4Cb	437.55049	93.27	1	i1807.5
15b	437.68725	93.27	1	i101.1
4Cc	457.06459	89.04	1	i1787.0
4Cd	480.66820	70.83	1	i1924.9
4Ce	383.41505	0.39	1	i516.2
HC(O)OH	186.21788		0	
MeF	137.16906	10.92 ^b	0	
NH ₂ F	152.87226	22.68 ^b	0	
HO ⁺ F	172.37421	26.06 ^b	0	(1573, 1698.0)
FF	195.98162	5.49 ^b	0	
HF	98.57285	11.27 ^b	0	

^a See footnote ^a to Table 1. ^b Relative energies of states with separate molecules of formic acid and the solvent (with no allowance for the superposition error^{1,12}).

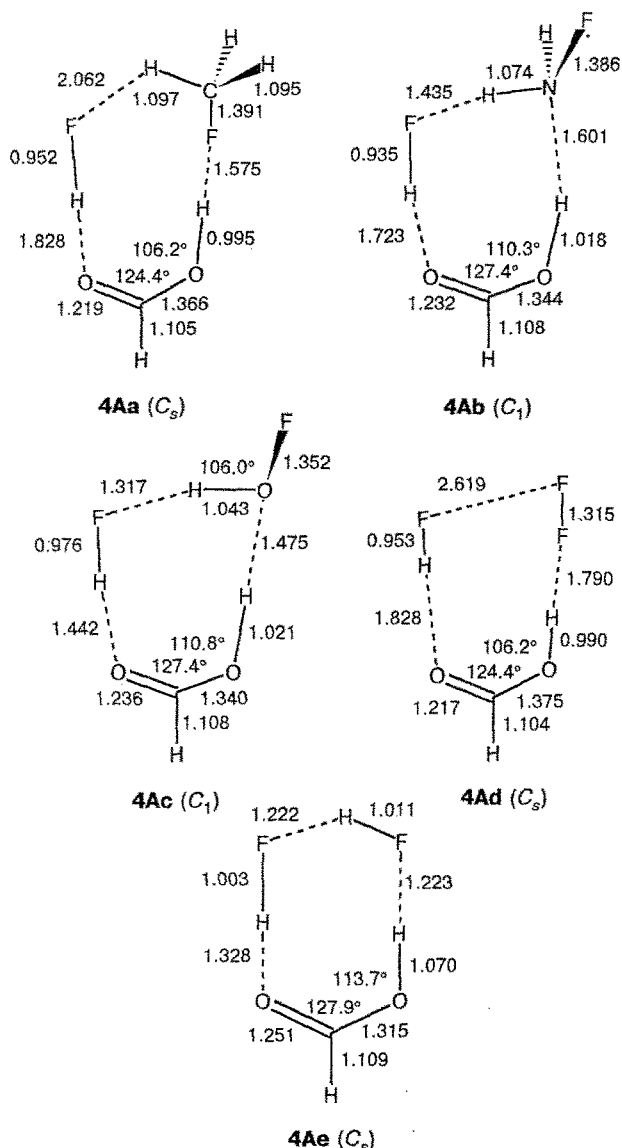


Fig. 4. Structures of associates **4A** calculated by the SCF/3G method. Bond lengths (in Å) and angles are presented.

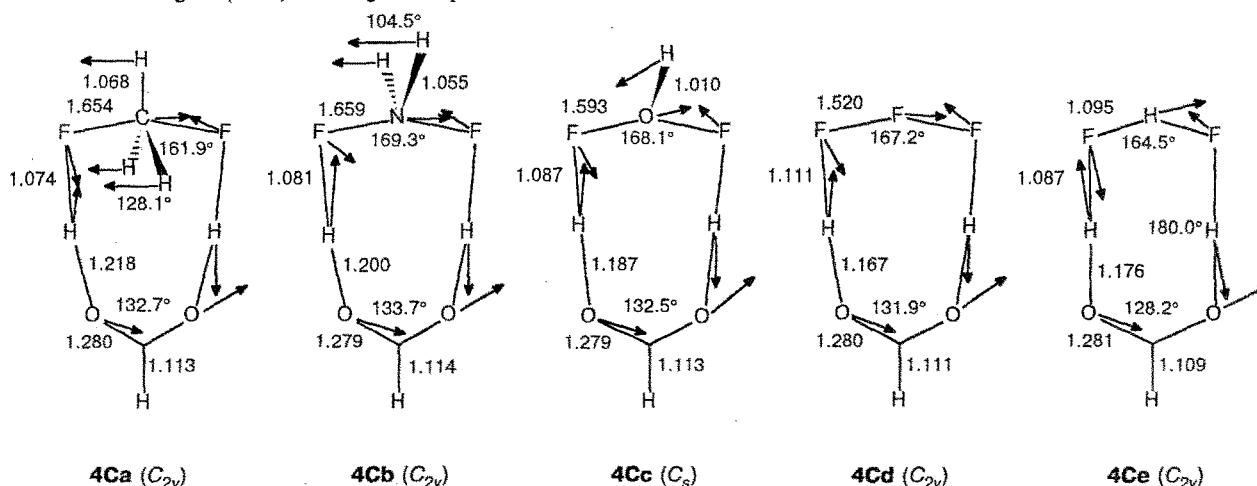


Fig. 5. Structures of transition states **4C** calculated by the SCF/3G method. Bond lengths (in Å) and angles are presented; the arrows denote components of the corresponding transient vectors.

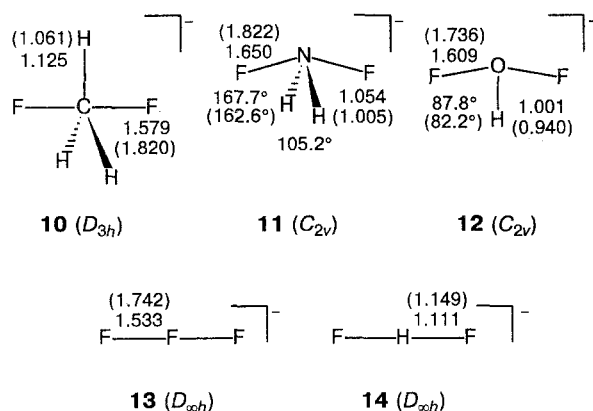
strong hydrogen bond between the molecules of fluoromethane and formic acid exists even in complex **4Aa** ($Y = \text{Me}$).

The 1,3-transfer of a proton, as in the previous case, proceeds *via* cyclic transition state **4C** with two bridging hydrogen bonds (see Fig. 5). In this reaction, two solvent molecules perform bifunctional (acid-base) catalysis; one of these acts as a proton donor, and the other acts as a proton acceptor. They simultaneously transport two protons along two hydrogen bridges, cooperatively with synchronous displacement of two F atoms. This process, like the previous one, can be conventionally divided into three "elementary" reactions: (a) transfer of a proton from the O atom of formic acid to the F atom of the FY molecule; (b) nucleophilic substitution of F at the central atom of the FY molecule; (c) transfer of a proton from the FY molecule to the second O atom of formic acid.

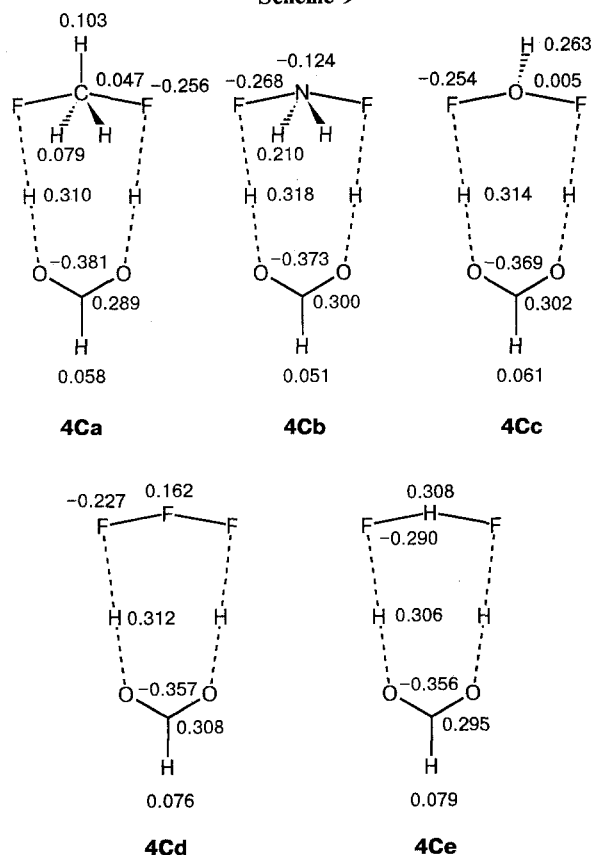
Transfer of a proton from one atom to another is governed by the same stereochemical requirements as that in the reaction presented in Scheme 3. The assignment of the second "elementary" reaction to bimolecular nucleophilic substitution (S_N2) of the F atom at the central atom of the FY molecule may be reasoned, first, by the fact that the configuration of the F—Y bonds at this atom in transition state **4C** is close to that found for the optimal structures of FCH_3F^- , FNH_2F^- , FOHF^- , FFF^- , and FHF^- (**10–14**, Scheme 8) modelling the simplest transition states of an S_N2 reaction involving period II atoms in the minimum STO-3G basis set,^{1,9} and, second, by the fact that both F atoms in structures **4C** carry rather large negative charges (Scheme 9, the numbers mean the charges of the corresponding atoms).

The bond lengths (in Å) and bond angles (see Scheme 8) in structures **10–14** calculated in the STO-3G approximation are compared to those calculated by higher-level methods (see numbers in parentheses). It can be seen that the nature of the stationary point on the PES and the geometry of the anion depend substantially on the calculation scheme. For example, *ab initio* SCF/DZP

Scheme 8



Scheme 9



calculations and higher-level calculations predict that structures **10**,²⁰ **11**,²¹ and **12** (our SCF/6-31G* calculation gave $E_{\text{total}} = -274.11685$ au, $\nu = 665.8$ cm⁻¹) are transition states ($\lambda = 1$), while **13**,^{22,23} and **14**,^{24,25} are the minima on the PES of the corresponding processes.

Species **10**–**12** have trigonal-bipyramidal structures in which unshared electron pairs act as phantom ligands. In this connection, anions **13** and **14**, by analogy with **10**–**12**, can be considered to be "elementary" transition structures in bimolecular nucleophilic substitution (S_N2)

at the F and H atoms (see Scheme 4). The trigonal-bipyramidal structure of the type **10** transition state of S_N2 processes at a saturated C atom has been rather well studied both experimentally^{1,9,26–28} and theoretically.^{1,12,20,29} The occurrence of an S_N2 reaction at a three-coordinated N atom *via* a type **11** transition state has been experimentally discovered recently^{26,30} and has been confirmed by high-level nonempirical calculations carried out for model systems.²¹ The stereochemistry of S_N2 reactions at two-coordinated O atoms and the T-shaped structure of transition state **12** predicted in our calculations are in good agreement with the previously obtained MINDO/3 data concerning the pathway of nucleophilic substitution at a peroxide oxygen atom³¹ and with the results of experimental studies of the kinetics of some reactions of peroxides.³² It is also well known^{1,9,22} that similar processes at an S atom proceed *via* a type **12** T-shaped transition state.

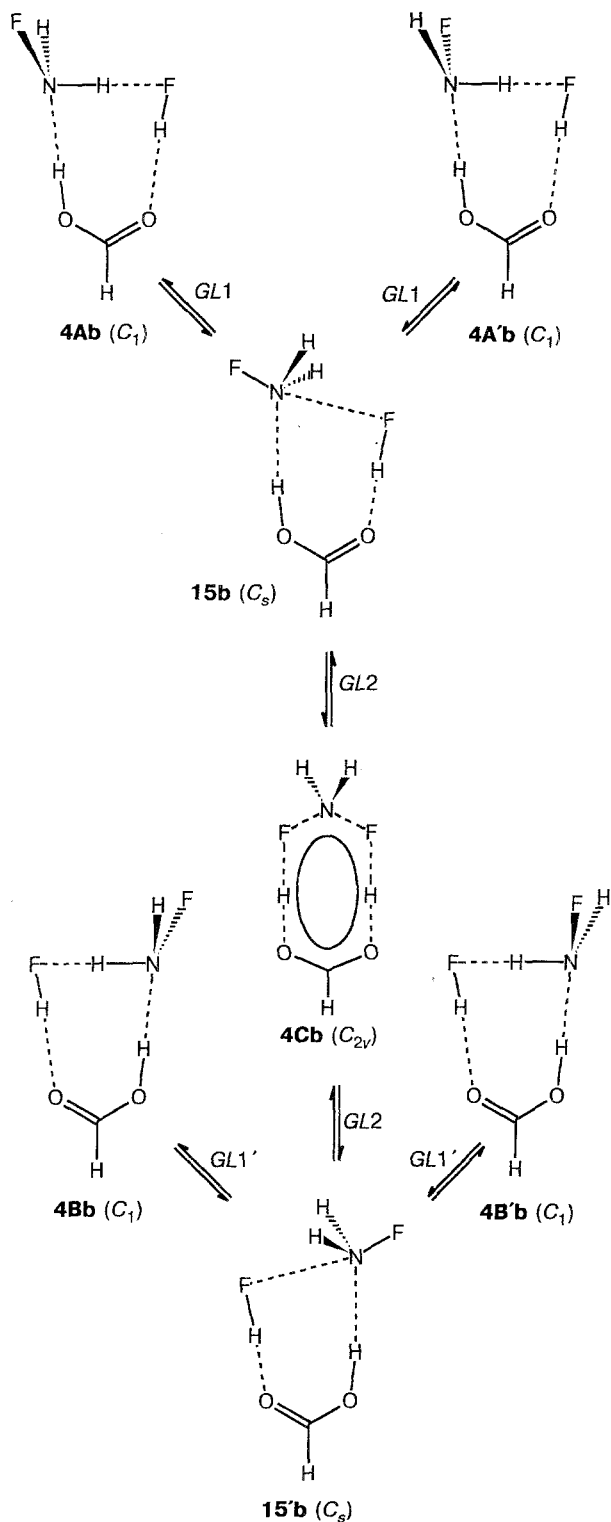
To the best of our knowledge, the pathway of bimolecular nucleophilic substitution at a F atom have not yet been experimentally or theoretically studied. However, it has been assumed²⁶ that intermolecular transfer of Br⁻ in some organic reactions occurs *via* type **13** linear transition state and can be regarded as an S_N2 process at the bromine atom. It is also noteworthy here that the existence of stable F–F–F⁻ anion is still a subject of discussion (see Refs. 22 and 23 and references in these papers).

The gradient pathway of the reaction shown in Scheme 4 is, as it usually is, unilinear for all of associates **4A**, except for **4Aa** and **4Ab**, and coincides with the optimized route¹ between the two minima, **4A** and **4B**, and transition state **4C**. However, this reaction pathway for associates **4Aa** and **4Ab** is complex (Scheme 10) and consists of three different gradient lines (*GL1*, *GL1'*, and *GL2*), two of which (*GL1* and *GL1'*) are equivalent and correspond to the reactions of **4Ab**, **4A'b** and **4Bb**, **4B'b**, i.e., transcoordination (1,3-shift) of the fluorine atom of the HF molecule with the YH molecule. Figure 6 presents two-dimensional schematic PES of system **4Ab** in the region of the configurational space corresponding to the **4A** = **4C** = **4B** reaction (see Schemes 4 and 10).

As can be seen, the gradient lines that connect the minima **4Ab** to **4A'b** and **4Bb** to **4B'b** pass through the points of transition structures **15b** and **15'b**, respectively. The *GL2* gradient line, which connects two transition states, **15b** and **15'b**, and passes through the third transition state, **4Cb**, reaches none of the minima. The transition vector of structure **4Cb** is smoothly transformed along the *GL2* gradient line into the Hessian eigenvector of associative form **15b** (or **15'b**), which corresponds to the minimum positive eigenvalue ($\nu_1 = 40.4$ cm⁻¹) and is perpendicular to the transition vector of this structure (**15b** or **15'b**).

Thus, the gradient reaction pathway changes its direction in the configurational space in the point of transition state **15b** (or **15'b**) and goes from the *GL2* line

Scheme 10



to $GL1$ (or $GL1'$). Both branches of the latter line lead to the minima corresponding to complexes $4Ab$ and $4A'b$ (or $4Bb$ and $4B'b$). Along the whole gradient reaction pathway from the saddle point ($4Cb$) to the minima ($4Ab$ and $4A'b$ or $4Bb$ and $4B'b$) via another

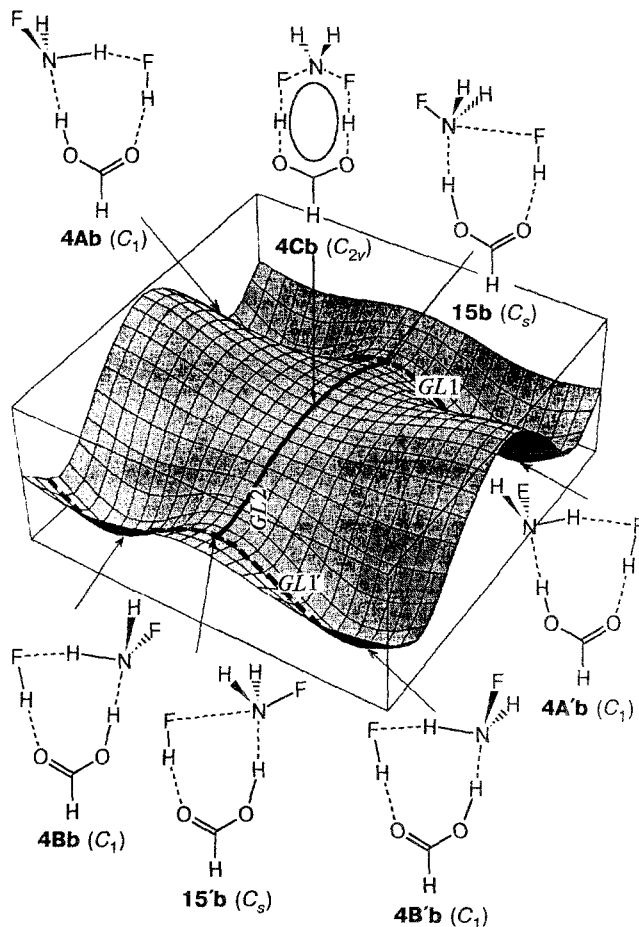


Fig. 6. Schematic view of the PES of system $4A$ in the region corresponding to the $4A \rightleftharpoons 4C \rightleftharpoons 4B$ reaction. The $GL2$ (solid) and $GL1$, $GL1'$ (dashed) bold-face lines are gradient reaction pathways.

saddle point ($15b$ or $15'b$), the total energy of the system continuously and smoothly decreases.

It is significant to note that on the $GL2$ line (on both sides from the point corresponding to transition state $4Cb$) bifurcation points³³ are located, where the "minimum-energy" pathway (but not the gradient line) splits off. In these points, the initial C_s symmetry of the molecular system is disrupted (the mirror symmetry plane disappears) and Pearson³⁴ or Pechukas³⁵ theorems for the minimum-energy pathway are not obeyed. However, on the gradient lines the point symmetry groups of the system, C_s on $GL2$ and C_1 on $GL1$ and $GL1'$, are retained from one critical point to another.³⁶

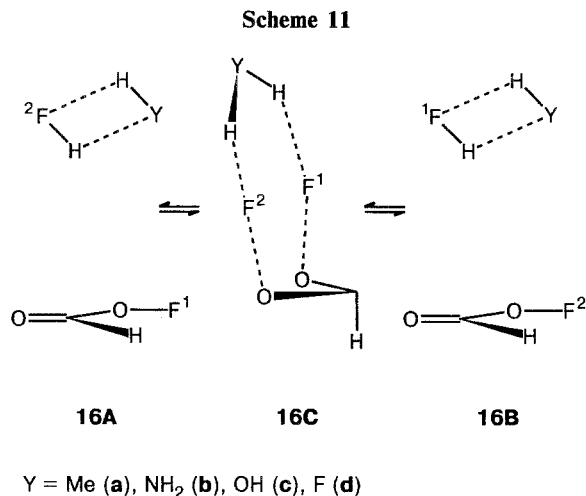
However, the bifurcation points are not critical (stationary), since the gradient does not disappear in these points ($\nabla E \neq 0$) and, hence, the gradient line cannot disappear or bifurcate. Since a chemical system can slide over the PES only along the gradient lines, structural instability appears in the bifurcation points, i.e., a shift in a direction perpendicular to $GL2$ results in a decrease in the total energy of the system.

The topology of the PES obtained for associates **4Aa** and **4Ab** in the region of configurational space corresponding to Scheme 10 is not unique and is probably quite common for other organic or inorganic processes. For example, this is true for bimolecular nucleophilic substitution in the $F^- \cdots NH_2F$ system (see Ref. 36) and it is also probably true for the inversion of the cyclooctatetraene ring and for its valence isomerization.³⁷ The PES of the H_2NSO_2OH molecule in the area of its isomerization³⁸ to the zwitterion form, $^+H_3N-SO_3^-$, has a similar structure.

The high activation barriers to the 1,3-shifts of protons calculated for associates **4Aa**, **4Ab**, **4Ac**, and **4Ad** indicate that the correspondence to the stereochemical requirements for the occurrence of "elementary" reactions in these systems is rather poor. In fact, as can be seen from Fig. 2, in structures **4C**, substantial deviations from the "ideal" stereochemistry, which predetermines the direction of the "elementary" reactions at each of the centers (bimolecular electrophilic substitution, S_E2 , at the F atom requires an angle configuration,¹ and for nucleophilic substitution, S_N2 , the linear $F-A-F$ fragment, where A is the central atom in the YF molecule,² is needed) and a substantial increase in the $O-C-O$ bond angle in the molecule of formic acid are observed. At the same time, the $4Ae \rightarrow 4Ce \rightarrow 4Be$ reaction is characterized by close stereochemical correspondence between the minimum-energy (**4A**) and transition (**4C**) structures and, consequently, by an extremely low activation barrier ($0.4 \text{ kcal mol}^{-1}$). Unlike the double transfer of protons in associates **3A**, the 1,3-shift of protons in systems **4A** in no case occurs by the mechanism of bimolecular electrophilic substitution of the F atom at the central atom of the solvent molecule, YF (F atoms, which are more electronegative than H atoms, cannot occupy equatorial positions at the central atom of the YF molecules in structures **4C**).

We have been interested in studying the peculiarities of the mechanism of the migration of groups in system **16A**, isomeric to **4A** (Scheme 11). Calculations show that structure **16Ca** corresponds to a transition state ($\lambda = 1$), **16Cb-d** correspond to intermediates ($\lambda = 0$), and **16A** corresponds to the dissociation of the system into a separate $HC(O)OF$ molecule and a hydrogen-bonded associate, $HF \cdots YF$. It should be noted that allowance for the superposition error in the calculation of the energies of stabilization of weakly bonded complexes may change substantially the obtained sequence of their thermodynamic stability.

Decomposition of transition structures (intermediates) **16C** occurs according to the following reaction pathway: YH and HF molecules move away from (approach) $HC(O)OF$, remaining in the same plane, perpendicular to the plane in which the molecule of formoxy fluoride lies (see Scheme 10). Figure 7 shows one of the forms that arise on the reaction pathway, when ammonia and hydrogen fluoride molecules approach formoxy fluoride. The energetic and geometric characteristics



calculated for systems **16A** and **16C** are presented in Figs. 7 and 8, respectively, and in Table 3.

The 1,3-shift of the F atom shown in Scheme 11 occurs *via* a cyclic chair-shaped transition (intermediate) state **16C** (see Fig. 8) with an extremely high activation barrier (see Table 3). As shown by calculations, planar structures **17C** are associated with the critical points with $\lambda \geq 3$ in the PES of the process, which is due to the antiaromatic nature of these structures. The antiaromatic nature (filling of antibonding π -MO) of associate **17C** governs the direction of the low-energy distortion of its planar structure, resulting in the chair-shaped form **16C** and in the stabilization of the antibonding π -MO filled with electrons (see **18** \rightarrow **19** in Scheme 12). This leads to a decrease in the total energy of the system and a variation of the index λ of the critical point for structure **16C** compared with **17C**.

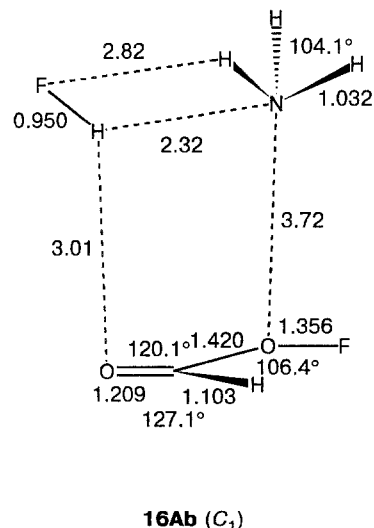


Fig. 7. SCF/3G-calculated structure of system **16Ab** with an energy of -437.66181 au , which arises on the reaction pathway when formoxy fluoride and HF and NH_3 molecules approach each other. Bond lengths (in Å) and angles are presented.

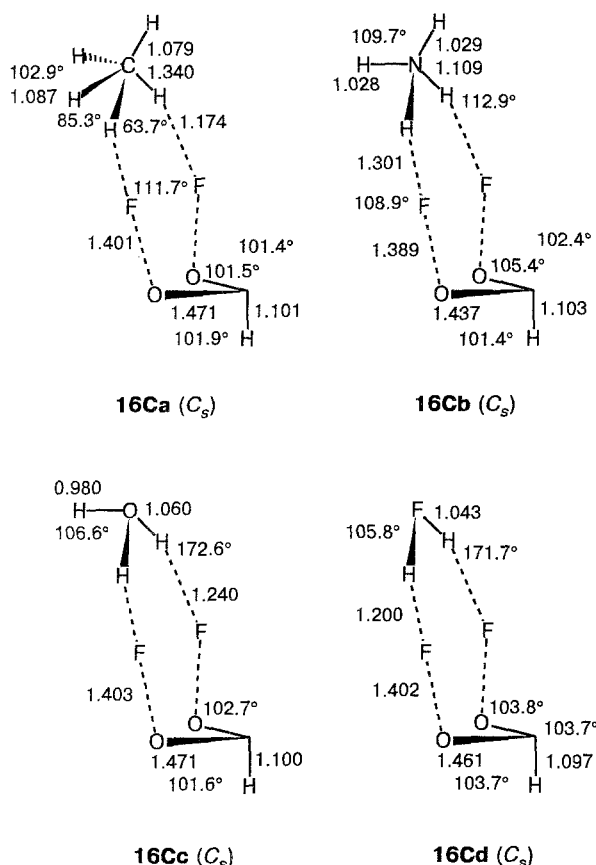
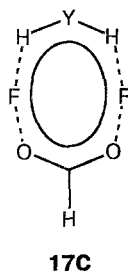


Fig. 8. Structures of transition states **16Ca** and **16Cc** and intermediates **16Cb** and **16Cd** calculated by the SCF/3G method. Bond lengths (in Å) and angles are presented.



Y = Me (**a**), NH_2 (**b**), OH (**c**), F (**d**)

Systems **16A** and **16C** are less energetically favorable (*cf.* Tables 2 and 3) than the corresponding isomeric structures **4A** and **4C**. This is caused by the fact that the O—F bond is much weaker than the O—H bond (so far no formoxy fluoride molecule has been experimentally detected, and its CH_3 - and CF_3 -substituted derivatives, $\text{H}_3\text{CC}(\text{O})\text{OF}$ ^{39,40} and $\text{F}_3\text{CC}(\text{O})\text{OF}$, ⁴¹ respectively, although having been detected in some studies, ^{39–41} are extremely unstable). However, formoxy fluoride is associated with a relatively deep minimum in the PES.

The SCF/3G-calculated geometric characteristics (bond lengths and angles) of the $\text{HC}(\text{O})\text{OF}$ and FOH

Table 3. Total (E_{total}) and relative (ΔE) energies, number of negative eigenvalues of Hessian (λ), and the two minimum (ν_1 , ν_2) or imaginary (iv) frequencies of systems **16A**, **16C** and molecules

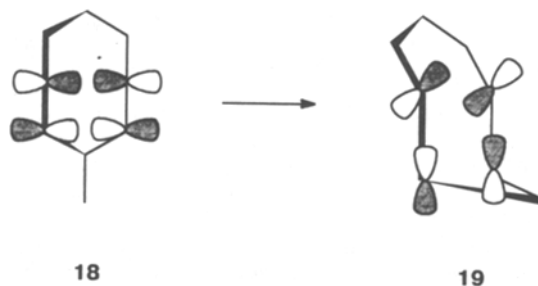
Structure	$-E_{\text{total}}$ /au	ΔE^a /kcal mol ⁻¹	λ	iv (ν_1 , ν_2) /cm ⁻¹
16Aa	421.92041 ^b	0		
16Ab	437.66181 ^b	0		
16Ac	457.17107 ^b	0		
16Ad	480.77483 ^b	0		
16Ca	421.66426	160.74	1	i2178.3
16Cb	437.55877	64.66	0	(87.6, 166.6)
16Cc	457.07115	62.70	0	(77.1, 183.5)
16Cd	480.67048	65.48	0	(113.5, 190.7)
$\text{HC}(\text{O})\text{OF}$	283.62036		0	(257.3; 313.0)
$\text{HF} \cdots \text{HCH}_3$	138.30008	0.36 ^c	—	
$\text{FH} \cdots \text{NH}_3$	154.04145	8.27 ^c	0	(241.8, 241.8)
$\text{FH} \cdots \text{OH}_2$	173.55071	7.51 ^c	0	(246.8, 253.6)
$\text{FH} \cdots \text{FH}$	195.98162	5.50 ^c	0	(262.7, 353.0)

^a See footnote ^a to Table 1. ^b Total energies of states with separate molecules of formoxy fluoride and hydrogen-bonded $\text{YH} \cdots \text{FH}$ system. ^c Relative energies of states with separate YH and FH molecules (with no allowance for the superposition error).

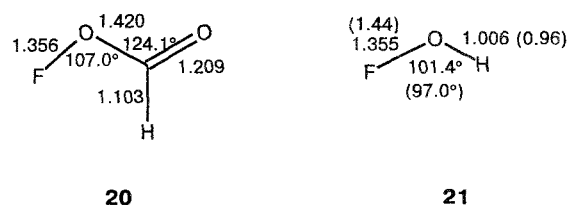
molecules are presented in Scheme 13, along with experimental data for FOH (see numbers in parentheses).

The lengths of the O—F bonds in compounds $\text{HC}(\text{O})\text{OF}$ and FOH predicted by *ab initio* (SCF/3G) calculations are shorter than those determined experimentally. ⁴² More exact agreement between the experimental and theoretical data for molecules incorporating O—F bonds can be achieved by using extended basis sets. ¹²

Scheme 12



Scheme 13



Thus, the calculations carried out imply that for low-barrier synchronized double proton transfer to occur, the principle of stereochemical correspondence must be fulfilled for all of the reaction contacts of the "elementary" steps in the given system: a nearly linear structure of the hydrogen bond bridge during the transfer of a proton and a structure close to the optimal structure of the transition states of S_N2 and S_E2 processes at the heavy atom of the solvent molecule (i.e., to a trigonal bipyramid for S_N2) as well as an angular configuration of the F atoms for the S_E2 reaction, are required. The height of the activation barrier in the case of associates **3** correlates with the electronegativity of the central atom of the solvent molecule, the mediator of the proton transfer.

The present work was carried out with financial support from the Russian Foundation for Basic Research (Project Nos. 93-03-4972 and 93-03-18692) and the International Science Foundation (Grant ISF RNJ 000).

References

1. V. I. Minkin, B. Ya. Simkin, and R. M. Minyaev, *Quantum Chemistry of Organic Compounds. Mechanisms of Reactions*, Springer-Verlag, Berlin, 1990, 270 pp.
2. W. J. Bouma, M. A. Vincent, and L. Radom, *Int. J. Quant. Chem.*, 1976, **14**, 767; M. R. Peterson and I. G. Csizmadia, *J. Am. Chem. Soc.*, 1979, **101**, 1076.
3. K. A. Nguyen, M. S. Gordon, and D. G. Truhlar, *J. Am. Chem. Soc.*, 1991, **113**, 1596.
4. K. Yamashita, M. Kaminoyama, T. Yamabe, and K. Fukui, *Theor. Chim. Acta*, 1986, **60**, 303.
5. M. Schlabach, H.-H. Limbach, E. Bunnenberg, A. Y. L. Shu, B.-K. Tolf, and C. Djerassi, *J. Am. Chem. Soc.*, 1993, **115**, 4554.
6. M. Schlabach, G. Scherer, and H.-H. Limbach, *J. Am. Chem. Soc.*, 1991, **113**, 3550.
7. S. Scheiner, *Acc. Chem. Res.*, 1985, **18**, 174; 1994, **27**, 402.
8. R. M. Minyaev and V. I. Minkin, *Dokl. Akad. Nauk*, 1995, **340**, 634 [*Dokl. Chem.*, 1995, **340** (Engl. Transl.)].
9. V. I. Minkin, L. P. Olekhovich, and Yu. A. Zhdanov, *Molecular Design of Tautomeric Compounds*, D. Reidel, Dordrecht—Boston—Tokyo, 1988, 271 pp.
10. F. Hibbert, *Adv. Phys. Org. Chem.*, 1986, **22**, 113.
11. G. G. Hammes, *Enzyme Catalysis and Regulation*, Academic Press, New York—London, 1982.
12. W. J. Hehre, L. Radom, P. v. R. Schleyer, and J. A. Pople, *Ab initio Molecular Orbital Theory*, J. Wiley & Sons, New York, 1986, 300 pp.
13. I. H. Williams, G. M. Maggiora, and R. L. Schowen, *J. Am. Chem. Soc.*, 1980, **102**, 7837.
14. R. D. Amos and S. M. Colwell, *MICROMOL*, Mark 5, University of Cambridge, Department of Theoretical Chemistry, Cambridge, 1988.
15. R. M. Minyaev, *Usp. Khim.*, 1994, **63**, 939 [*Russ. Chem. Rev.*, 1994, **63** (Engl. Transl.)].
16. N. Shida, P. F. Barbara, and J. Almlof, *J. Chem. Phys.*, 1991, **94**, 3633.
17. H.-B. Burgi and J. Dunitz, *Acc. Chem. Res.*, 1983, **16**, 153.
18. M. C. Etter, *J. Phys. Chem.*, 1991, **95**, 4601.
19. D. V. Gurvich, G. V. Karachevtsev, V. N. Kondrat'ev, Yu. A. Lebedev, V. A. Medvedev, V. E. Potapov, and Yu. S. Khodeev, *Energii razryva khimicheskikh svyazei. Potentsialy ionizatsii i srodstvo k elektronu* [The Energies of Cleavage of Chemical Bonds. Ionization Potentials and Electron Affinity], Nauka, Moscow, 1974, 351 pp. (in Russian).
20. S. Wolfe, D. J. Mitchel, and H. B. Schlegel, *J. Am. Chem. Soc.*, 1981, **103**, 7692.
21. M. Bühl and H. F. Schaefer, *J. Am. Chem. Soc.*, 1993, **115**, 364, 9143.
22. G. L. Heard, C. J. Marsden, and G. E. Scuseria, *J. Phys. Chem.*, 1992, **96**, 4359.
23. K. O. Christe and W. W. Wilson, *J. Am. Chem. Soc.*, 1992, **114**, 9934.
24. S. Gronet, *J. Am. Chem. Soc.*, 1993, **115**, 10258.
25. K. Luth and S. Scheiner, *Int. J. Quant. Chem., Quant. Chem. Sympos.*, 1992, **26**, 817.
26. P. Beak, *Acc. Chem. Res.*, 1992, **25**, 215.
27. C. C. Han, J. A. Dodd, and J. I. Brauman, *J. Phys. Chem.*, 1986, **90**, 471.
28. S. E. Barlow, J. M. van Doren, and V. M. Bierbaum, *J. Am. Chem. Soc.*, 1980, **102**, 7240.
29. R. Vetter and L. Zülke, *J. Am. Chem. Soc.*, 1990, **112**, 5136.
30. P. Beak and J. Li, *J. Am. Chem. Soc.*, 1991, **113**, 2796.
31. R. M. Minyaev and M. E. Kletskii, *Teor. Eksp. Khim. [Theor. and Experim. Chem.]*, 1980, **16**, 368 (in Russian).
32. E. N. Prilezhaeva, *Reaktsiya Prilezhaeva. Elektrofilynoe okislenie* [Prilezhaev Reaction. Electrophilic Oxidation], Nauka, Moscow, 1974, 331 pp. (in Russian).
33. M. V. Basilevsky, *Chem. Phys.*, 1977, **24**, 81.
34. R. G. Pearson, *Theor. Chim. Acta*, 1970, **16**, 107.
35. P. Pechukas, *J. Chem. Phys.*, 1976, **64**, 1516.
36. R. M. Minyaev and D. J. Wales, *Zh. Organ. Khim.*, 1995, **34** (in press) [*Russ. J. Org. Chem.*, 1995, **34** (Engl. Transl.)].
37. D. A. Hrovat and W. T. Borden, *J. Am. Chem. Soc.*, 1992, **114**, 5879.
38. M. W. Wong, K. B. Wieberg, and M. J. Frisch, *J. Am. Chem. Soc.*, 1992, **114**, 523.
39. S. Rozen, O. Lerman, and M. Kol, *J. Chem. Soc., Chem. Comm.*, 1981, 443.
40. E. H. Appelman, M. H. Mendelsohn, and H. Kim, *J. Am. Chem. Soc.*, 1985, **107**, 6515.
41. G. H. Cady and K. B. Kellogg, *J. Am. Chem. Soc.*, 1953, **75**, 2501.
42. A. F. Wells in *Structural Inorganic Chemistry*, 2, 5th Ed., Oxford Univ. Press, Oxford (England), 1986.

Received March 27, 1995